Rock Mechanics and Rock Engineering (2022) 55:1571–1582
https://doi.org/10.1007/s00603-021-02738-y

ORIGINAL PAPER

A New Rock Brittleness Index Based on the Peak Elastic Strain Energy Consumption Ratio

Fengqiang Gong[1,2] · **Yunliang Wang**[3]

Received: 10 August 2021 / Accepted: 5 December 2021 / Published online: 20 January 2022

Abstract

To evaluate rock brittleness more accurately, a new rock brittleness index based on the peak elastic strain energy consumption ratio (PEECR) was proposed in this study. Considering the relationship between rock brittleness and energy evolution characteristics of rock materials under confining pressure, the PEECR was defined as the dissipated proportion of peak elastic strain energy relative to failure energy and residual elastic strain energy (the maximum value of PEECR is 1.0, which indicates the corresponding rock will fail immediately after reaching the peak strength). The evaluation accuracy of the PEECR was verified based on the conventional triaxial compression tests on shale under six confining pressures, and the universality of the PEECR was also analyzed according to test data of six types of rocks from previous studies. The results show that the PEECR continuously decreases with the increasing of confining pressures, and is suitable for various types of rocks and a wider range of brittleness degrees. Finally, the evaluation accuracies of the PEECR and 11 existing rock brittleness energy indexes were compared and analyzed, and the results indicate that PEECR can evaluate rock brittleness more accurately.

Highlights

- A new rock brittleness index based on peak elastic strain energy consumption ratio (PEECR) was proposed considering the relationship between the rock brittleness and energy evolution characteristics of rock materials under confining pressures.
- It is verified based on conventional triaxial compression tests that PEECR can accurately evaluate rock brittleness, and is suitable for various types of rocks and a wider range of brittleness degrees.
- The evaluation accuracy for rock brittleness of PEECR is higher than other existing indexes by comparison based on test results, and PEECR can be popularized in practical application.

Keywords Rock brittleness index · Shale brittleness · Energy evolution characteristics · Peak elastic strain energy consumption ratio

✉ Fengqiang Gong
fengqiangg@126.com

[1] Engineering Research Center of Safety and Protection of Explosion and Impact of Ministry of Education (ERCSPEIME), Southeast University, Nanjing 211189, China

[2] School of Civil Engineering, Southeast University, Nanjing 211189, China

[3] School of Resources and Safety Engineering, Central South University, Changsha 410083, China

List of Symbols

BI_{ER}	Peak elastic strain energy consumption ratio
E	Pre-peak elastic modulus
σ_1	Axial stress
σ_3	Circumferential stress
σ_p	Peak strength
σ_r	Residual strength
ε_d	Axial strain when peak stress is unloaded to 0
ε_r	Axial strain at the beginning point of residual strength stage
ε_u	Axial strain when the residual stress is unloaded to 0
ε_p	Peak axial strain

U^{e}_{p} Peak elastic strain density
U^{f} Failure energy density
U^{e}_{r} Residual elastic strain energy density
U^{a} Additional input energy density
U^{ec} Consumed elastic strain energy density during the failure process
U^{d}_{p} Peak dissipated energy density
U^{ei} Peak elastic strain energy of the absolute brittle rock

1 Introduction

Brittleness is an essential property of rock, and has great impact on the rock failure characteristics. There are numerous practical engineering problems that are closely related to rock brittleness. Brittleness is a key factor for evaluating the hydraulic fracturing feasibility in unconventional energy development (such as shale gas and geothermal energy) (Jarvie et al. 2007; Guo et al. 2015; Lai et al. 2015; Zhang et al. 2016; Meng et al. 2021; Wang et al. 2021). The determination of technical parameters of hydraulic fracturing largely depends on rock brittleness. Therefore, it is crucial to have a better understanding of rock brittleness and accurately evaluate the degree of brittleness.

To evaluate the rock brittleness, numerous brittleness indexes have been proposed based on various aspects (Meng et al. 2021), including mineral compositions (Guo et al. 2015; Kim et al. 2017; Shi et al. 2017; Huo et al. 2018; Moghadam et al. 2019), mechanical parameters (Hucka and Das 1974; Khandelwal et al. 2017), stress–strain curves characteristics (Hajiabdolmajid and Kaiser 2003; Gong and Sun 2015; Meng et al. 2015; Shi et al. 2019; Kuang et al. 2021), conventional well logging (Suorineni et al. 2009; Tang et al. 2016; Kaunda and Asbury 2016), internal friction angle (Hucka and Das 1974; Zhou et al. 2018), penetration tests (Copur et al. 2003; Yagiz 2009), indentation tests (Hucka and Das 1974; Lawn and Marshall 1979; Fan et al. 2019), content of fines after impact (Hucka and Das 1974), and energy evolution characteristics (Tarasovn and Randolph 2011; Tarasovn and Potvin 2013; Ai et al. 2016; Xia et al. 2017; Kivi et al. 2018; Song et al. 2019; Li et al. 2019a, b, 2020; Zhang et al. 2021). Further researches indicated that the deformation and failure of rock is always accompanied by the storage, dissipation, transformation, and release of energy, and rock failure is essentially the destabilizing phenomenon driven by energy (Xie et al. 2008). Moreover, some researchers believe that the increasing tendency of rock plasticity can be regarded as the gradual growing effect of energy dissipation mechanism (Chen et al. 2015), which means that the brittleness of rock is related to energy dissipation. On this basis, an increasing number of scholars have focused on studying the energy evolution characteristics during the process of rock deformation and failure to obtain accurate evaluation methods of rock brittleness, and various brittleness indexes have been proposed from different perspectives. The existing 11 rock brittleness indexes based on energy are summarized in Table 1 including their definitions and characteristics.

According to the analyses in Table 1, all the mentioned existing rock brittleness indexes based on energy have some defects, which affect their evaluation accuracy. Therefore, it is necessary to propose a more scientific and precise rock brittleness index. In this study, the relationship between the energy evolution characteristics of rock deformation and the failure process and rock brittleness was deeply analyzed to propose a more accurate rock brittleness index. The reliability of the new index was then verified based on conventional triaxial compression tests. The evaluation accuracy of the new index and existing indexes was compared and analyzed.

2 A New Rock Brittleness Index Based on Energy: Peak Elastic Strain Energy Consumption Ratio

To propose a new rock brittleness index based on energy that can accurately evaluate rock brittleness, the energy evolution characteristics of the entire rock deformation and failure process were analyzed first. The actual stress–strain curve of a rock conventional triaxial compression test is shown in Fig. 1a, based on which a sketch of the energy evolution characteristics of the rock deformation and failure process is presented in Fig. 1b. During the pre-peak stage, input energy was transformed into two forms (it is presumed that there is no heat exchange with outside) (Xie et al. 2008). One (elastic strain energy) of them is stored in rock, which will be released if the stress on rocks is unloaded; it is also the driving energy for the failure of rock. The other one (dissipated energy) is dissipated due to the damage and plastic deformation of rock. When rock reaches its energy storage limitation, it will begin to fail. A part of the accumulated elastic strain energy will induce the failure of rock, another part will dissipate due to the damage of rock, and the residual part has two different states for different loading conditions. For uniaxial loading conditions, the residual elastic strain energy will mainly transform into the kinetic energy for rock fragments ejection. With regard to triaxial compression condition, the rock will reach its residual strength stage, and the residual elastic strain energy will store in the rock.

According to the analyses of energy evolution characteristics and the test results of rocks with different brittleness degrees from previous studies (Ai et al. 2016; Xia et al. 2017; Kivi et al. 2018; Song et al. 2019; Li et al. 2019a, b, 2020), it is found that the energy evolution characteristic of the post-peak rock failure process is crucial to the rock brittleness degree, and it is believed that the brittler the rocks are, the less pre-peak stored elastic strain energy will transform into failure

Table 1 Eleven existing rock brittleness indexes based on energy

Rock brittleness indexes	Energy parameters	Characteristics
$BI_1 = \frac{U_p^e}{U_p^e + U_p^d}$ (Hucka and Das 1974)	U^a, U^f and U_c^e are the additional input energy, total failure energy and consumed elastic strain energy during the failure process, respectively U_p^e, U_p^d and U_r^e are the peak elastic strain energy, peak dissipated energy and residual elastic strain energy, respectively σ_p and σ_r are the peak strength and residual strength, respectively U^{ei} is the peak elastic strain energy of the absolute brittle rock	BI_1 means that the more elastic strain energy is stored in rock during pre-peak stage, the more brittle the rock is. However, the post-peak energy evolution characteristic is not considered in this index, which also has a great impact on rock brittleness
$BI_2 = \frac{U^f}{U_c^e}$ (Tarasovn and Randolph 2011; Tarasovn and Potvin 2013) $BI_3 = \frac{U^a}{U_c^e}$ (Tarasovn and Randolph 2011; Tarasovn and Potvin 2013)		BI_2 implies post-peak energy evolution characteristics, the failure relies more on the elastic strain energy and less on additional input energy, the more brittle the rock is.BI_3 means the less additional input energy is needed and the more stored elastic strain energy is consumed during the failure process, the more brittle the rock is. However,BI_2 and BI_3 are simplified as the relationship of the pre-peak elastic modulus and post-peak deformation modulus in original article, which will definitely affect the judgment accuracy
$BI_4 = \frac{U^f + U_p^d}{U_c^e + U_p^d}$ (Ai et al. 2016) $BI_5 = \frac{U^a}{U_c^e + U_p^d}$ (Ai et al. 2016)		BI_4 involves the impact of the pre-peak dissipated energy on the brittleness comparing with BI_2. It is believed that the less dissipated energy is generated during the pre-peak, the more brittle the rock is. BI_5 signifies dissipated energy has a negative influence on the rock brittle failure. However, the formulas of BI_4 and BI_5 are unsuitable and paradoxical
$BI_6 = \frac{1}{2}\left(\frac{U_c^e}{U^f} + \frac{U_c^e}{U_p^e + U_p^d}\right)$ (Kivi et al. 2018)		BI_6 was proposed considering both the pre-peak and post-peak energy evolution characteristics. It is believed that more elastic strain energy is stored in the pre-peak stage and used for failure in the post-peak stage, the rock is more brittle. Despite this index is considered comprehensively, there is still a problem: the fracture energy should be the area under the post-peak curve subtracting the residual elastic strain energy, but the fracture energy in this index also includes the peak elastic strain energy
$BI_7 = \frac{U^a}{U_c^e} + \frac{U_p^e + U_p^d}{U_p^e}$ (Song et al. 2019)		BI_7 means that the more stored elastic strain energy is consumed and less additional input energy is needed during the failure process, the more brittle the rock is
$BI_8 = \frac{U_p^e}{U_p^e + U_p^d} \times \frac{U_c^e}{U^f} \times \left(1 - \frac{U_r^e}{U_p^e}\right)$ (Li et al. 2019a)		BI_8 considers the impact of residual elastic strain energy on brittleness. It is believed that the bigger proportion of the stored elastic strain energy is consumed for failure and the smaller is left, the more brittle the rock is
$BI_9 = \frac{U_p^e}{U_p^e + U_p^d} \times \frac{U_c^e}{U^f}$ (Li et al. 2019a)		BI_9 is extremely similar to BI_6; they have the same physical meanings. However, BI_9 is expressed in the form of multiplication
$BI_{10} = \frac{U_p^e}{U_p^e + U_p^d} \times \left(1 - \frac{U_p^d}{U_p^d + U^f}\right) \frac{\sigma_p - \sigma_r}{\sigma_p}$ (Li et al. 2019b)		BI_{10} involves the dissipation rate of the failure energy. It is believed that the faster the failure energy is dissipated, the more brittle the rock is. However,BI_7,BI_8,BI_9 and BI_{10} all join different factors with multiplication which lacks a theoretical basis
$BI_{11} = \frac{U_p^e}{U^{ei}} \times \frac{U^f}{U^a}$ (Li et al. 2020)		BI_{11} means the input energy will totally transfer into elastic strain energy for the absolute brittle rock, and the more elastic strain energy is stored in the rock, the more brittle the rock is. However, the calculation method of the elastic strain energy for ideal brittle rocks was not verified and thus not convincing

energy and less residual elastic strain energy will still store in rocks. Moreover, for rocks with higher brittleness, the failure energy is provided by the pre-peak stored elastic strain energy; with regard to the rocks of lower brittleness, rock failure is induced by the pre-peak elastic strain energy and post-peak additional input energy.

On this basis, a new brittleness index called the peak elastic strain energy consumption ratio was proposed, and the formula is as follows:

$$\mathrm{BI}_{\mathrm{ER}} = \frac{U_{\mathrm{p}}^{\mathrm{e}} - U^{\mathrm{f}} - U_{\mathrm{r}}^{\mathrm{e}}}{U_{\mathrm{p}}^{\mathrm{e}}}, \tag{1}$$

where $U_{\mathrm{p}}^{\mathrm{e}}$ is the peak elastic strain density, U^{f} is the failure energy density, and $U_{\mathrm{r}}^{\mathrm{e}}$ is the residual elastic strain energy density ($U_{\mathrm{r}}^{\mathrm{e}}=0$ under uniaxial compression conditions for brittle rocks, but $U_{\mathrm{r}}^{\mathrm{e}}$ also exists for some soft rocks even under uniaxial compression). The larger the value of $\mathrm{BI}_{\mathrm{ER}}$ is, the brittler the rock is. When $\mathrm{BI}_{\mathrm{ER}}=1$ (the maximum value of $\mathrm{BI}_{\mathrm{ER}}$), the rock is extremely brittle. When $\mathrm{BI}_{\mathrm{ER}}$ is smaller, more $U_{\mathrm{p}}^{\mathrm{e}}$ is needed during failure process, and the plasticity of rock is higher. Specially, if $\mathrm{BI}_{\mathrm{ER}}<0$, $U_{\mathrm{p}}^{\mathrm{e}}$ is not enough to maintain rock failure, additional input energy is needed in the post–peak stage, and the rocks like this are usually more plastic than the general rocks. Therefore, it is believed that the newly proposed $\mathrm{BI}_{\mathrm{ER}}$ can reflect a wide range of rock brittleness degree variations. To verify the reliability and universality of $\mathrm{BI}_{\mathrm{ER}}$, a series of laboratory tests were conducted.

3 Verification of the Reliability and Universality of $\mathrm{BI}_{\mathrm{ER}}$

In general, conventional triaxial compression (CTC) tests are used when rock brittleness is assessed by related brittleness indexes, and it is believed that the brittleness of the same type of rock will decrease with increasing confining pressures (Chen et al. 2017; Meng et al. 2020). Therefore, the evaluation accuracy of rock brittleness indexes can be judged by the variation trends of the index values under different confining pressures. To verify the reliability and accuracy of $\mathrm{BI}_{\mathrm{ER}}$, a series of CTC tests were conducted in this study.

3.1 Conventional Triaxial Compression Tests

A type of shale from Sichuan Province, China was selected for the tests. The shale was processed into standard cylindrical specimens (φ50 mm × 100 mm) (Fig. 2), and the bedding dip angle of the specimens is 0°. The basic parameters of the shale specimens are shown in Table 2. The tests were carried out based on the MTS 815 rock mechanics test system (Fig. 3). The maximum axial load of the system is 2600 kN, and its confining pressure can reach 140 MPa. The axial and circumferential strain of the specimens are measured by an axial and circumferential extensometer, respectively.

Before the CTC tests, a conventional uniaxial compression (UC) test (i.e., the confining pressure is 0 MPa) was first conducted on a specimen for comparison, and the loading rate was 0.05 MPa/s with stress control. In the CTC tests, the axial and circumferential stresses were loaded on the specimens simultaneously at a rate of 0.05 MPa/s (stress control mode), and then, the circumferential stress was kept at the preset confining pressures (5 MPa, 10 MPa, 20 MPa, 30 MPa, 50 MPa, 70 MPa); the axial stress was loaded continuously until the specimens failed. The loading paths of CTC tests are shown in Fig. 4. Six specimens were applied to complete the tests under six confining pressures as described above.

After the tests, a series of stress–strain curves were obtained (Fig. 5). It is known that there are four regions during the pre-peak stage for common curves (Cai et al. 2004, 2021; Jaeger et al. 2007): microcrack closure compaction region (the original microcracks of rocks are gradually closed, the rocks are compacted), elastic deformation region (the curve is almost a straight line), stable microcrack growth region (the microcracks stably grow), and unstable microcrack propagation region (the rocks show ductility and the microcracks in rocks violently grow until the rocks totally fail). It can be observed in Fig. 5 that the microcrack closure compaction region and elastic deformation region are obvious, but the stable microcrack growth and unstable microcrack propagation regions are almost nonexistent for the specimens under the confining pressures of 0 MPa, 5 MPa, and 10 MPa, which indicates that specimens under these conditions show high brittleness. With regard to the specimens under 20 MPa and 30 MPa, the microcrack closure compaction region is nearly disappearing, but the stable microcrack growth region is more obvious, which means that the brittleness of the specimens gradually decrease. For the rocks under 50 MPa and 70 MPa, the unstable microcrack propagation region is more evident, indicating that the brittleness of specimens further declines. The above analysis shows that the brittleness of specimens gradually decreases with the increasing of confining pressures, which accords with the regular situations (Chen et al. 2017; Meng et al. 2020). Moreover, the peak strength and residual strength increased with increasing confining pressures, which is consistent with the results of previous studies (Ai et al. 2016; Xia et al. 2017; Kivi et al. 2018; Song et al. 2019; Li et al. 2019a, b, 2020; Yang et al. 2020). This indicates that more pre-peak elastic strain energy is needed for failure and that more elastic strain energy is preserved in the specimen after failure with increasing confining pressures.

Fig. 1 The actual axial stress–strain curve of conventional triaxial compression tests and a sketch of energy evolution characteristics during the rock deformation and failure process based on the corresponding simplified curve (σ_p is peak strength, σ_r is residual strength, ε_d is the axial strain when the stress of ideal unloading curve is 0, ε_r is the residual axial strain, ε_u is the axial strain when the stress of ideal post-peak unloading curve is 0, ε_p is the peak axial strain,σ_1 is the axial stress, σ_3 is the circumferential stress.)

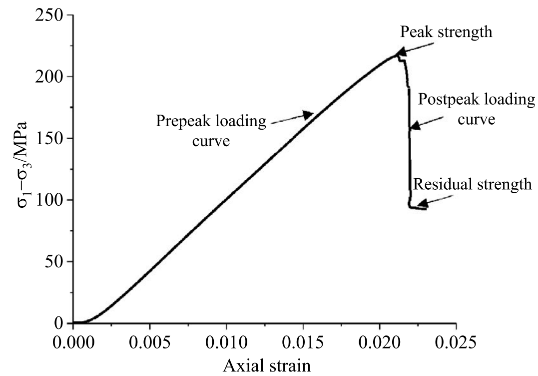

(a) Axial stress-strain curve of shale specimens from conventional triaxial compression tests under a confining pressure of 20 Mpa

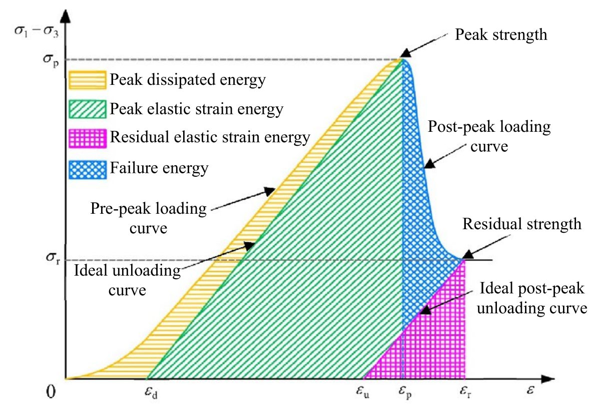

(b) Sketch of the energy evolution characteristics during the rock deformation and failure process (Tarasovn and Randolph 2011)

3.2 *Verification of the Reliability of* $\mathrm{BI_{ER}}$ *for Rock Brittleness Evaluation*

Based on the obtained stress–strain curves, $\mathrm{BI_{ER}}$ can be used to evaluate the brittleness of the tested shale specimens under different confining pressures. The calculation methods of the energy density parameters in $\mathrm{BI_{ER}}$ are shown as follows (Xie et al. 2008; Tarasovn and Randolph 2011; Tarasovn and Potvin 2013; Ai et al. 2016):

$$U_p^e = \frac{\sigma_c^2}{2E} \tag{2}$$

$$U_r^e = \frac{\sigma_r^2}{2E} \tag{3}$$

when $\varepsilon_p < \varepsilon_u$,

$$U^f = \int_{\varepsilon_p}^{\varepsilon_r} \sigma d\varepsilon - U_r^e \tag{4}$$

when $\varepsilon_p > \varepsilon_u$,

$$U^f = \int_{\varepsilon_p}^{\varepsilon_r} \sigma d\varepsilon - U_r^e + \frac{1}{2}(\varepsilon_p - \varepsilon_u)^2 \times E \tag{5}$$

where E is the pre-peak elastic modulus; it is the tangent modulus, which is defined as the slope of the straight portion of pre-peak curve. With regard to ε_p, ε_u, and ε_u, as shown in Fig. 1b, ε_p is the axial strain corresponding to the peak strength point; ε_r is the axial strain corresponding to the beginning point of residual strength stage; ε_u is the axial strain when the stress of the ideal post-peak unloading curve is 0; the ideal post-peak unloading curve is a straight line from the beginning point of residual strength stage, which is parallel to the straight portion of pre-peak loading curve.

The brittleness evaluation results of $\mathrm{BI_{ER}}$ for the tested shale specimens under different confining pressures (0 MPa, 5 MPa, 10 MPa, 20 MPa, 30 MPa, 50 MPa, 70 MPa) were obtained according to the above curves, as shown in Table 3. The relationship between $\mathrm{BI_{ER}}$ of the specimens and the corresponding confining pressures is shown in Fig. 6. It can be observed that the values of $\mathrm{BI_{ER}}$ decline continuously with increasing confining pressures. As mentioned above, the smaller $\mathrm{BI_{ER}}$ is, the less brittle the rock is; the rock brittleness will be lower with increasing confining pressures. Therefore, it can be concluded

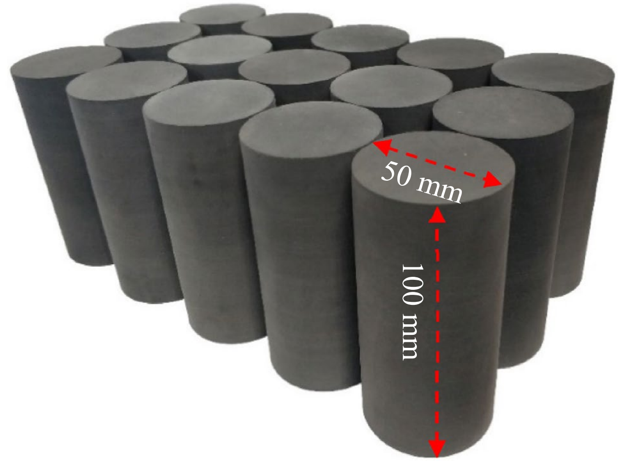

Fig. 2 The processed shale specimens

Table 2 The basic parameters of shale specimens

Density/ ($g \cdot cm^{-3}$)	P-wave velocity/ ($m \cdot s^{-1}$)	Elastic modulus/ GPa	Uniaxial compressive strength/MPa
2.49	4074.27	19.17	167.65

that BI_{ER} can accurately evaluate rock brittleness. Moreover, the above results are consistent with the characteristics of the pre-peak stress–strain curves of shale under different confining pressures in Fig. 5: the brittleness of rocks is higher under the confining pressures of 0 MPa, 5 MPa, and 10 MPa; the brittleness of rocks gradually decreases under 20 MPa and 30 MPa; the brittleness of rocks is lower under 50 MPa and 70 MPa.

3.3 Verification of the Universality of BI_{ER}

To verify the universality of BI_{ER}, the test data of other studies (Xia et al. 2017; Kivi et al. 2018; Li et al. 2019b; Kuang et al. 2021) were cited, six types of rocks were subjected to CTC tests in these studies, and the corresponding stress–strain curves are shown in Fig. 7. BI_{ER} was applied to evaluate the brittleness of these rocks, and the results are shown in Table 4. To intuitively analyze the evaluation accuracy of BI_{ER}, the relationships between BI_{ER} and the corresponding confining pressures are shown in Fig. 8. It can be observed that the values of BI_{ER} decrease as the confining pressures increase, which indicates that the evaluation results for the six types of rocks by BI_{ER} are accurate, and BI_{ER} is reliable. Specifically, some BI_{ER} values are negative (Table 4), which means that the corresponding rocks are more ductile, the peak elastic strain energy is not sufficient to maintain rock failure, and additional input energy is needed. Therefore, it can be concluded that BI_{ER} is suitable for various types of rocks and a wider range of brittleness degrees.

4 Discussion

A new rock brittleness index BI_{ER} based on energy was proposed in this study. This index considers the relationship between rock brittleness and the energy evolution characteristics of the entire deformation and failure process of rocks, is defined in a scientific form, and it can accurately evaluate the brittleness of various types of rocks. It is believed that BI_{ER} is reliable and exhibits superiority.

To further verify its superiority, the evaluation accuracy of BI_{ER} was compared with 11 existing rock brittleness indexes based on energy. Eleven existing rock brittleness indexes are summarized in Table 1, including their definitions and physical meanings. BI_{ER} and the summarized 11 indexes were used to

Fig. 3 MTS 815 rock mechanics test system

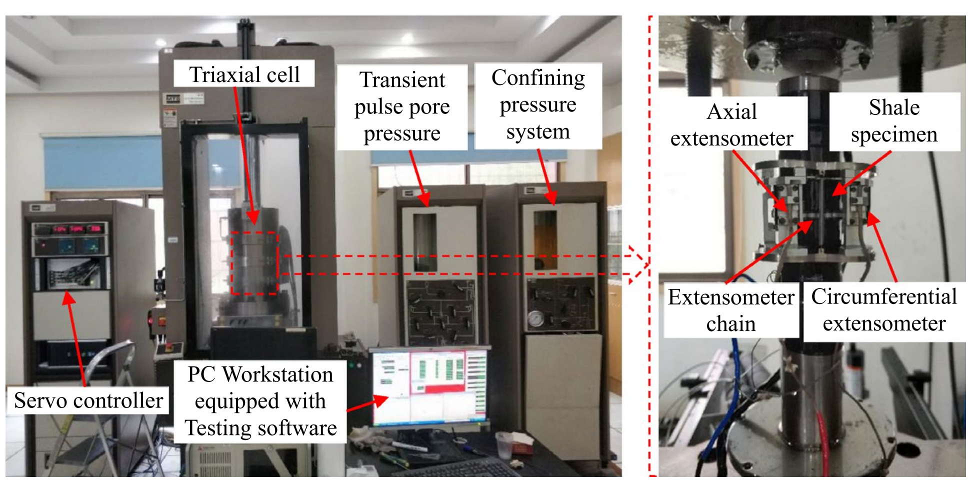

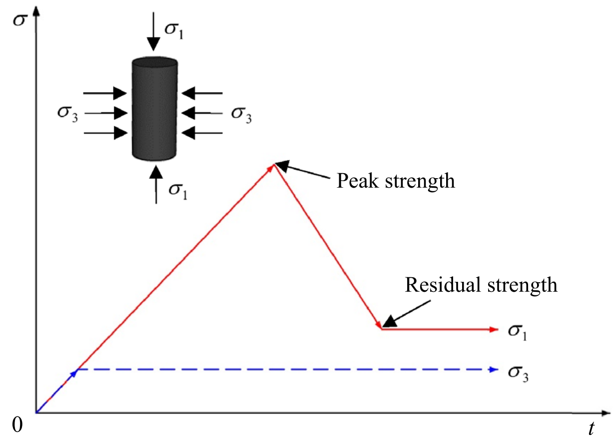

Fig. 4 Loading path of CTC tests

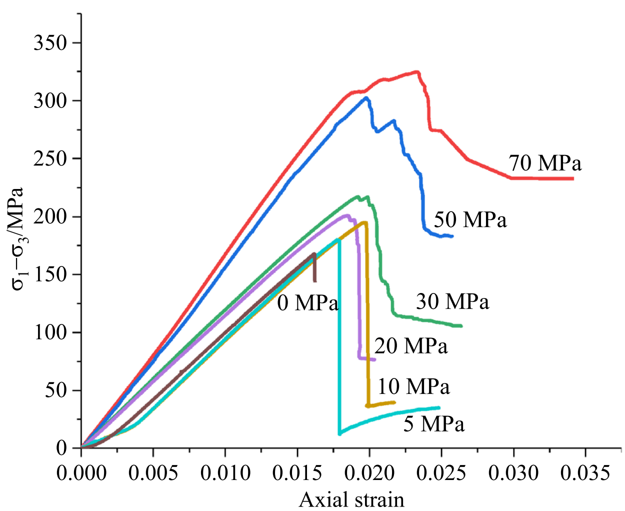

Fig. 5 Shale specimens stress–strain curves of the UC tests and CTC tests under six confining pressures

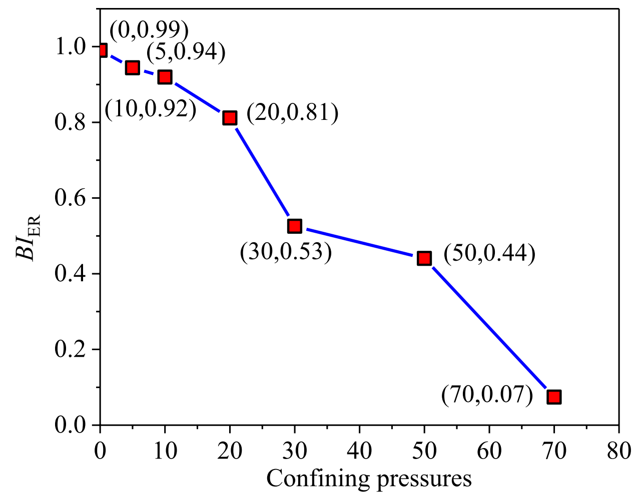

Fig. 6 The relationship between BI_{ER} of the tested shale specimens and the corresponding confining pressures

evaluate the brittleness of the shale specimens under six confining pressures of the above CTC tests (Sect. 3.1) to compare their brittleness evaluation accuracy. The evaluation results of these indexes for specimens under different confining pressures are shown in Fig. 9.

It can be observed that the values of indexes (except for BI_{ER}) exhibit fluctuations with increasing confining pressures, and they do not increase or decrease continuously, which indicates that these indexes cannot accurately evaluate rock brittleness. With regard to BI_{ER}, its values decline continuously with the increasing of confining pressures. Therefore, it can be concluded that BI_{ER} exhibits superiority, and can evaluate rock brittleness more accurately.

Actually, the indexes involved in Fig. 9 are relatively accurate for rock brittleness evaluation in the particular fields, but there is not a unified judgment standard for their accuracies. Under this circumstance, the evaluation accuracies of them can only be judged according to the qualitative trend that the rock brittleness continuously decreases with the increasing of confining pressures, as shown in Fig. 9.

Furthermore, it should be noted that the calculation methods of peak elastic strain energy and residual elastic strain

Table 3 BI_{ER} of the tested shale specimens of the UC tests and CTC tests under six confining pressures

Confining pressure /MPa	Peak strength/MPa	Residual strength/MPa	U_p^e(mJ/mm^3)	U^f(mJ/mm^3)	U_r^e(mJ/mm^3)	BI_{ER}
0	167.65	0	0.9031	0.0094	0	0.99
5	179.98	34.79	1.3565	0.0314	0.0446	0.94
10	194.76	39.43	1.6149	0.1194	0.0107	0.92
20	200.91	76.64	2.5481	0.2339	0.2463	0.81
30	217.01	105.66	1.9992	0.9208	0.0283	0.53
50	302.48	184.99	2.7151	1.1764	0.3428	0.44
70	324.79	249.04	2.8126	1.7203	0.8840	0.07

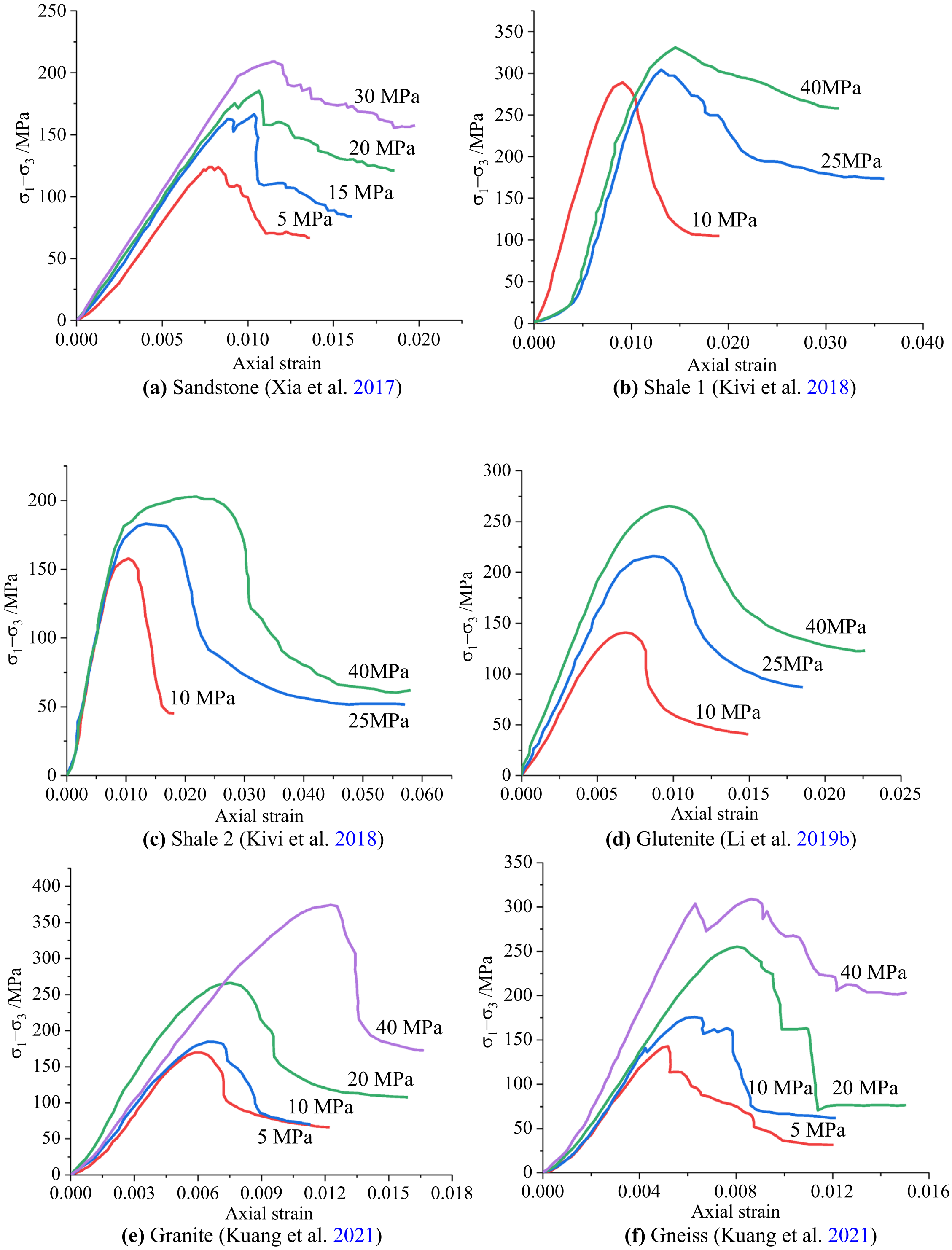

Fig. 7 Stress–strain curves of six types of rocks (Kuang et al. 2021; Xia et al. 2017; Kivi et al. 2018; Li et al. 2019b)

Table 4 The evaluation results of the six types of rocks by BI_{ER}

Rock type	Confining pressure/MPa	Peak strength/MPa	Residual strength/MPa	BI_{ER}
Sandstone (Xia et al. 2017)	5	135.30	65.10	0.55
	15	166.80	81.40	− 0.16
	20	173.30	107.30	− 0.31
	30	181.40	129.40	− 1.10
Shale 1 (Kivi et al. 2018)	10	299.60	107.20	− 0.46
	25	331.20	194.30	− 1.54
	40	370.50	258.20	− 3.69
Shale 2 (Kivi et al. 2018)	10	168.40	50.10	− 0.19
	25	209.40	63.10	− 2.58
	40	244.40	71.20	− 2.76
Glutenite (Li et al. 2019a, b)	10	141.13	46.12	− 0.34
	15	214.37	89.09	− 0.81
	20	265.16	126.04	− 1.08
Granite (Kuang et al. 2021)	5	171.31	94.223	0.57
	10	183.84	87.873	0.52
	20	266.18	118.96	0.41
	40	374.93	185.41	0.37
Gneiss (Kuang et al. 2021)	5	142.44	50.84	− 0.11
	10	175.83	67.1	− 0.20
	20	255.43	77.07	− 0.32
	40	308.26	202.71	− 0.46

energy as shown in Eqs. (2) and (3) are approximate methods, whose results definitely exist errors form the actual values. The previous studies (Gong et al. 2018, 2019, 2021, 2022; Li and Gong (2020); Su et al. 2021) indicate that the linear energy storage law exists in rocks, coals and concretes of pre-peak stage under one-dimensional, two-dimensional, and three-dimensional loading conditions. Therefore, the further work of this research is to obtain three-dimensional compression energy storage coefficient by cyclic loading and unloading triaxial compression tests, obtain the accurate calculation method of peak elastic strain energy and residual elastic strain energy, and modify peak elastic strain energy consumption ratio.

5 Conclusion

To propose a more accurate rock brittleness index, the relationship between energy evolution characteristics under confining pressure and rock brittleness of rock materials was analyzed, and the reliability of the new index was verified based on a series of CTC tests on shale. The main conclusions are as follows:

1. A new rock brittleness index BI_{ER} was proposed based on the peak elastic strain energy consumption ratio, which considers the correlation between the entire energy evolution process of rocks and brittleness and is defined in a scientific form.
2. A series of CTC tests were conducted to verify the reliability of BI_{ER}, and the results show that BI_{ER} can accurately evaluate rock brittleness. Moreover, the CTC test data of various types of rocks under different confining pressures of previous studies were cited to verify the universality of BI_{ER}, whose result indicates that BI_{ER} is suitable for various types of rocks and a wider range of brittleness degrees.

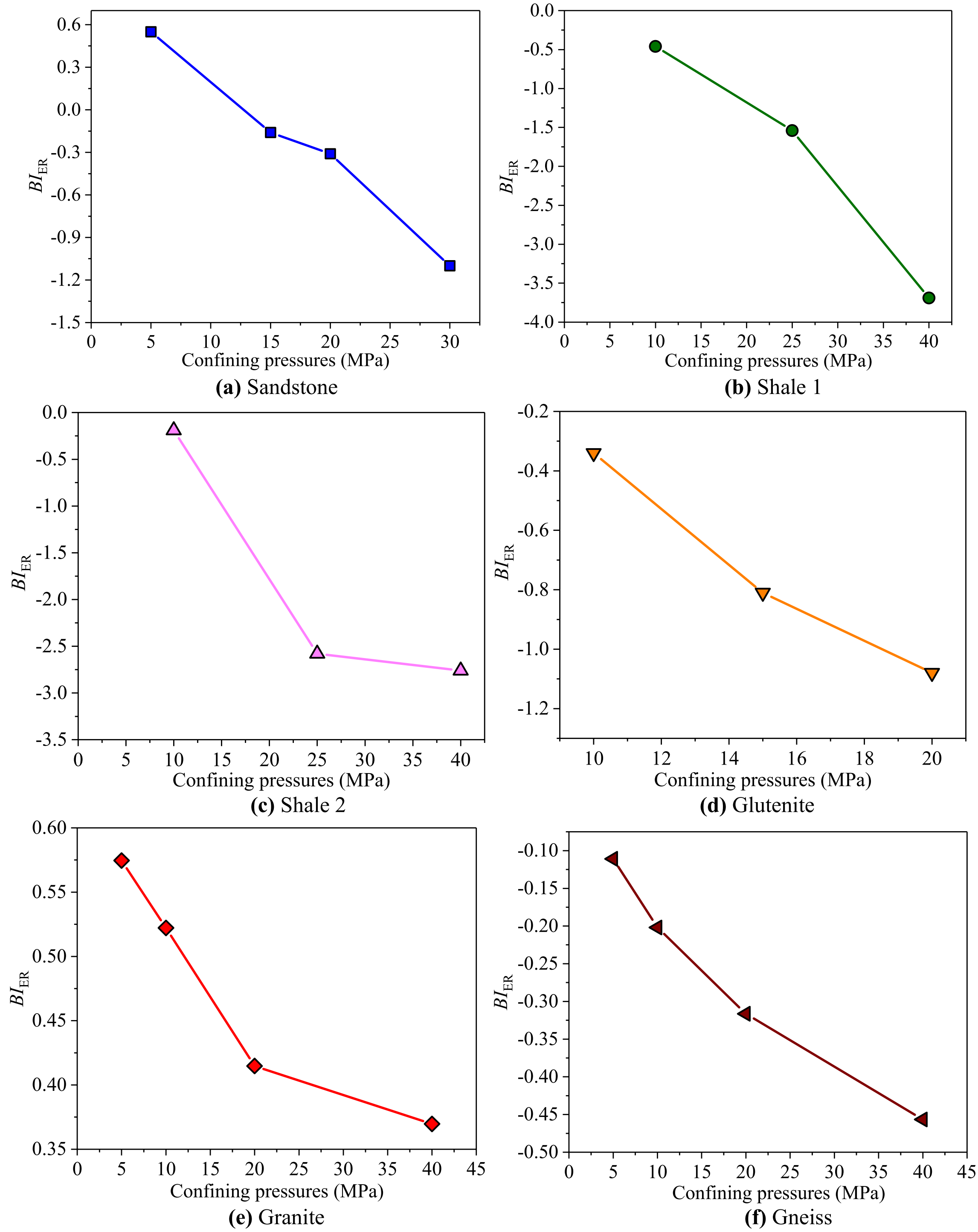

Fig. 8 The relationship between BI_{ER} and the corresponding confining pressures

3. The evaluation results of BI_{ER} and 11 existing brittleness indexes for shale brittleness under six confining pressures were compared, and the result shows that BI_{ER} can evaluate rock brittleness more accurately.
4. BI_{ER} is clearly defined and its form is simple. Its calculation process is also very convenient and can be popularized in practical application.

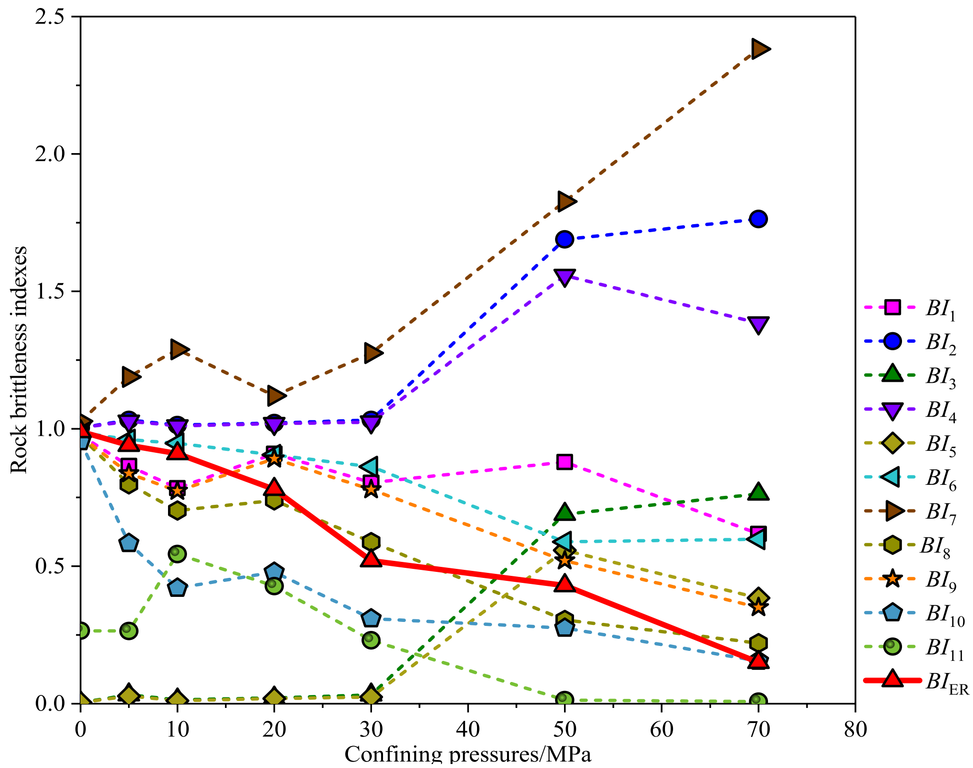

Fig. 9 Evaluation results of 11 existing brittleness indexes and BI_{ER} for shale specimens under six confining pressures

Acknowledgements This work was supported by the National Natural Science Foundation of China (Grant No. 42077244) and the Fundamental Research Funds for the Central Universities of Southeast University (Grant No. 2242021R10080, 3205002108C3).

References

Ai C, Zhang J, Li YW, Zeng J, Yang XL, Wang JG (2016) Estimation criteria for rock brittleness based on energy analysis during the rupturing process. Rock Mech Rock Eng 49:4681–4698

Cai M, Kaiser PK, Tasaka Y, Maejima T, Morioka H, Minami M (2004) Generalized crack initiation and crack damage stress thresholds of brittle rock masses near underground excavations. Int J Rock Mech Min Sci 41:833–847

Cai M, Hou PY, Zhang XW, Feng XT (2021) Post-peak Stress-Strain curves of brittle hard rocks under axial-strain-controlled loading. Int J Rock Mech Min Sci 147:104921

Chen Y, Jin Y, Chen M (2015) A rock brittleness evaluation method based on energy dissipation. Chin J Theor Appl Mech 47(6):984–993

Chen Y, Jin Y, Chen M, Yi ZC, Zheng XJ (2017) Quantitative evaluation of rock brittleness based on the energy dissipation principle, an application to type II mode crack. J Nat Gas Sci Eng 45:527–536

Copur H, Bilgin N, Tuncdemir H, Balci C (2003) A set of indices based on indentation tests for assessment of rock cutting performance and rock properties. J South Afr Inst Min Metall 103(9):589–599

Fan M, Jin Y, Chen M, Geng Z (2019) Mechanical characterization of shale through instrumented indentation test. J Pet Sci Eng 174:607–616

Gong X, Sun CC (2015) A new tablet brittleness index. Eur J Pharm Biopharm 93:260–266

Gong FQ, Yan JY, Li XB (2018) A new criterion of rock burst proneness based on the linear energy storage law and the residual elastic energy index. Chin J Rock Mech Eng 37(9):1993–2014

Gong FQ, Yan JY, Luo S, Li XB (2019) Investigation on the linear energy storage and dissipation laws of rock materials under uniaxial compression. Rock Mech Rock Eng 52:4237–4255

Gong FQ, Wang YL, Wang ZG, Pan JF, Luo S (2021) A new criterion of coal burst proneness based on the residual elastic strain energy index. Int J Min Sci Technol 31(4):553–563

Gong FQ, Shi RH, Xu L (2022) Linear energy storage and dissipation laws of concrete under uniaxial compression at different ages. Constr Build Mater 318:125963. https://doi.org/10.1016/j.conbuildmat.2021.125963

Guo TK, Zhang SC, Ge HK, Wang XQ, Lei X, Xiao B (2015) A new method for evaluation of fracture network formation capacity of rock. Fuel 140:778–787

Hajiabdolmajid V, Kaiser P (2003) Brittleness of rock and stability assessment in hard rock tunnelling. Tunn Undergr Space Technol 18:35–48

Hucka V, Das B (1974) Brittleness determination of rocks by different methods. Int J Rock Mech Min Sci Geomech Abstr 11(10):389–392

Huo ZP, Zhang JC, Li P, Tang X, Yang X, Qiu QL, Dong Z, Li Z (2018) An improved evaluation method for the brittleness index of shale and its application—A case study from the southern north China basin. J Nat Gas Sci Eng 59:47–55

Jaeger JC, Cook NG, Zimmerman R (2007) Fundamentals of rock mechanics, 4th edn. Blackwell Publishing, Malden

Jarvie DM, Hill RJ, Ruble TE, Pollastro RM (2007) Unconventional shale-gas systems: the Mississippian Barnett Shale of northcentral Texas as one model for thermogenic shale-gas assessment. AAPG Bull 91(4):475–499

Kaunda RB, Asbury BP (2016) Prediction of rock brittleness using nondestructive methods for hard rock tunneling. J Rock Mech Geotech Eng 8(4):533–540

Khandelwal M, Faradonbeh RS, Monjezi M, Armaghani DJ, Majid MZ (2017) Function development for appraising brittleness of intact rocks using genetic programming and non-linear multiple regression models. Eng Comput 33(1):13–21

Kim T, Hwang S, Jang S (2017) Petrophysical approach for S-wave velocity prediction based on brittleness index and total organic carbon of shale gas reservoir: a case study from Horn River Basin, Canada. J Appl Geophys 136:513–520

Kivi IR, Ameri M, Molladavoodi H (2018) Shale brittleness evaluation based on energy balance analysis of stress-strain curves. J Pet Sci Eng 167:1–19

Kuang ZH, Qiu SL, Li SJ, Du SH, Huang Y, Chen XQ (2021) A new rock brittleness index based on the characteristics of complete stress-strain behaviors. Rock Mech Rock Eng 54:1109–1128

Lai J, Wang GW, Huang LX, Li WL, Ran Y, Wang D, Zhou ZL, Chen J (2015) Brittleness index estimation in a tight shaly sandstone reservoir using well logs. J Nat Gas Sci Eng 27:1536–1545

Lawn BR, Marshall DB (1979) Hardness, toughness, and brittleness: an indentation analysis. J Am Ceram Soc 62(7–8):347–350

Li LL, Gong FQ (2020) Experimental investigation on the energy storage characteristics of red sandstone in triaxial compression tests with constant confining pressure. Shock Vib 10:1–11

Li N, Zou YS, Zhang SC, Ma XF, Zhu XW, Li SH, Cao T (2019a) Rock brittleness evaluation based on energy dissipation under triaxial compression. J Pet Sci Eng 183:1–10

Li LC, Zhai MY, Zhang LY, Zhang ZL, Huang B, Li AL, Zuo JQ, Zhang QS (2019b) Brittleness evaluation of glutenite based on energy balance and damage evolution. Energies 12(18):1–28

Li YW, Zhou LH, Li DP, Zhang SC, Tian FC, Xie ZM, Liu B (2020) Shale brittleness index based on the energy evolution theory and evaluation with logging data: a case study of the Guandong block. ACS Omega 5:13164–13175

Meng FZ, Zhou H, Zhang CQ, Xu RC, Lu JJ (2015) Evaluation methodology of brittleness of rock based on post-peak stress–strain curves. Rock Mech Rock Eng 48:1787–1805

Meng QB, Wang CK, Huang BX, Pu H, Zhang ZZ, Sun W, Wang J (2020) Rock energy evolution and distribution law under triaxial cyclic loading and unloading conditions. Chin J Rock Mech Eng 39(10):2047–2059

Meng FZ, Wong LNY, Zhou H (2021) Rock brittleness indices and their applications to different fields of rock engineering: a review. J Rock Mech Geotech Eng 13(1):221–247

Moghadam A, Harris NB, Ayranci K, Gomez JS, Angulo NA, Chalaturnyk R (2019) Brittleness in the Devonian Horn River shale, British Columbia, Canada. J Nat Gas Sci Eng 62:247–258

Shi X, Wang J, Ge XM, Han ZY, Qu GZ, Jiang S (2017) A new method for rock brittleness evaluation in tight oil formation from conventional logs and petrophysical data. J Pet Sci Eng 151:169–182

Shi GC, Chen G, Pan YT, Yang XL, Liu Y, Dai GZ (2019) Stress-drop effect on brittleness evaluation of rock materials. J Cent South Univ 26(7):1807–1819

Song HQ, Zuo JP, Chen Y, Li LY, Hong ZJ (2019) Revised energy drop coefficient based on energy characteristics in whole process of rock failure. Rock Soil Mech 40(1):91–98

Su YQ, Gong FQ, Luo S, Liu ZX (2021) Experimental study on energy storage and dissipation characteristics of granite under two-dimensional compression with constant confining pressure. J Cent South Univ 28:848–865

Suorineni FT, Chinnasane DR, Kaiser PK (2009) A procedure for determining rock-type specific Hoek-Brown brittle parameter s. Rock Mech Rock Eng 42(6):849–881

Tang XM, Xu S, Zhuang C, Su YD, Chen XL (2016) Quantitative evaluation of rock brittleness and fracability based on elastic-wave velocity variation around borehole. Pet Explor Dev 43(3):457–464

Tarasovn BG, Potvin Y (2013) Universal criteria for rock brittleness estimation under triaxial compression. Int J Rock Mech Min Sci 59:57–69

Tarasovn BG, Randolph MF (2011) Superbrittleness of rocks and earthquake activity. Int J Rock Mech Min Sci 48:888–898

Wang SF, Tang Y, Wang SY (2021) Influence of brittleness and confining stress on rockcuttability based on rock indentation tests. J Cent South Univ 28(9):2786–2800

Xia YJ, Li LC, Tang CA, Li XY, Ma S, Li M (2017) A new method to evaluate rock mass brittleness based on stress–strain curves of class I. Rock Mech Rock Eng 50:1123–1139

Xie HP, Ju Y, Li LY, Peng RD (2008) Energy mechanism of deformation and failure of rock mass. Chin J Rock Mech Eng 27(9):1729–1740

Yagiz S (2009) Assessment of brittleness using rock strength and density with punch penetration test. Tunn Undergr Space Technol 24(1):66–74

Yang SQ, Yin PF, Ranjith PG (2020) Experimental study on mechanical behavior and brittleness characteristics of Longmaxi Formation Shale in Changning, Sichuan Basin, China. Rock Mech Rock Eng 53:2461–2483

Zhang D, Ranjith PG, Perera MSA (2016) The brittleness indices used in rock mechanics and their application in shale hydraulic fracturing: a review. J Pet Sci Eng 143:158–170

Zhang Y, Feng XT, Yang CX, Han Q, Wang ZF, Kong R (2021) Evaluation method of rock brittleness under true triaxial stress states based on pre-peak deformation characteristic and post-peak energy evolution. Rock Mech Rock Eng 54:1277–1291

Zhou H, Chen J, Lu JJ, Jiang Y, Meng FZ (2018) A new rock brittleness evaluation index based on the internal friction angle and class I stress-strain curve. Rock Mech Rock Eng 51:2309–2316